Visualization of Age-Dependent Circadian Changes in Autonomic Drive on Heart Rhythm by Network Representation of RR-increments

Danuta Makowiec[1], Zbigniew R. Struzik[2,3,1]

[1] Institute of Theoretical Physics and Astrophysics, Gdansk University, Poland
[2] RIKEN, Brain Science Institute, Japan
[3] Graduate School of Education, University of Tokyo, Japan

Abstract

A method is presented which is capable of detailed characterization of the transition probability structure of heart period rhythm. The method is applied to two parts of the Holter recordings, diurnal and nocturnal, of healthy individuals grouped according to their age and gender. It reveals and quantifies patterns of short-term dynamics. This geometrically oriented approach provides a plausible method for distinguishing between healthy and pathological variability.

1. Introduction

It is believed that changes in heart rhythm result from the constant control maintained by the autonomic nervous system [1]. However, different mechanisms are responsible for heart accelerations and decelerations. Adjustments caused by the sympathetic part of the autonomic regulation are slow — on a scale of seconds — whereas adjustments by the vagal part of this regulation are an order of magnitude faster [2]. We, therefore, focus on the qualification and quantification of heart accelerations and decelerations in order to gain insight into the particular mechanisms driving short-term heartbeat dynamics across circadian activities: diurnal and nocturnal.

Network representations of time series [3, 4] are used to explore dynamic relationships between values of RR-intervals, *i.e.* time intervals between consecutive normal-to-normal heart contractions.

2. Methods

2.1. Data acquisition

Twenty-four-hour Holter ECG recordings during a normal sleep-wake cycle were obtained from healthy volunteers without any known cardiac history. The signals were grouped according to their age and gender: *young* — 15 females, 15 males (age: 19...25), and *elderly* — 11 females, 11 males (age: 70...89).

Holter recordings were first analyzed using Del Mar Reynolds Impresario software and screened for premature, supraventricular and ventricular beats, missed beats and pauses. Then the signals were thoroughly corrected manually and annotated correspondingly.

The hours of sleep were identified for each signal individually in order properly to detect the day-night transition. A six-hour period, covering the longest RR-intervals, was extracted as the nocturnal period. The diurnal rhythm was analyzed using a three-hour period from 16:00 to 19:00 hours. Perturbations in signals — artifacts or not normal-to-normal RR-intervals — consisting of less than five consecutive RR-intervals were replaced by the median estimated from the previous seven normal RR-intervals. Other perturbations were deleted. Ultimately, the nocturnal signals were constructed from at least 20 000 RR-intervals, and the diurnal from at least 12 000 RR-intervals.

2.2. State space of of RR-increments

Let $\mathbf{RR} = \{RR_0, \ldots, RR_i, \ldots, RR_N\}$ denote a time sequence of RR-intervals with time index i. The signal of RR-increments is defined as $\mathbf{\Delta RR} = \{\delta RR_1, \ldots, \delta RR_i, \ldots, \delta RR_N\}$ with $\delta RR_i = RR_i - RR_{i-1}$. If $\delta RR_i < 0$, we have an acceleration; if $\delta RR_i > 0$, we have a deceleration; and if $\delta RR_i = 0$, we call this a no-change event.

The Holter equipment provided data with a 128 Hz sampling frequency, which settled the resolution of RR-intervals at 8 ms. Therefore all the values of RR-intervals obtained, and in consequence of the RR-increments, are multiples of 8 ms: $0, \pm 8, \pm 16, \ldots$. These values, arranged from the largest acceleration to the largest deceleration, are referred to as labels for the states of the state space. Thus if $\Delta_K = \max_i\{|\delta RR_i|\}$, the state space consists of 2K+1 states denoted as follows:

$$\Delta_J \in \{-\Delta_K, \ldots, -8, 0, 8, \ldots, \Delta_K\}. \qquad (1)$$

2.3. Transition network representation

The transition network of $\mathbf{\Delta RR}$ is a graph of all pairs $(\delta RR_i, \delta RR_{i+1})$ in the state space described by 1. The vertices are labelled by values of 1 and each pair $(\delta RR_i, \delta RR_{i+1})$ enters a directional edge connecting the corresponding states. Since the same values occur many times, all these edges are expressed by a single weighted edge. Hence, for the construction of the graph, we count events which are equal to a given pair (Δ_I, Δ_J), with $I, J = 1, \ldots 2K+1$ of all possible combinations of the states described by (1).

The network graph can be represented a square matrix $\mathbf{A}$, called adjacency matrix, of size $(2K+1)$ with entries $A_{I,J} = P(\Delta_I, \Delta_J)$, describing probabilities that events (Δ_I, Δ_J) occur as a consecutive temporal sequence.

The deceleration capacity DC [5], obtained by the phase-rectified signal averaging method (PRSA), follows the events described by a deceleration at time i :

$$\frac{1}{4}(RR_i + RR_{i+1} - RR_{i-1} - RR_{i-2}),$$

which can be rewritten as

$$\frac{1}{4}(\delta RR_{i-1} + \delta RR_i + \delta RR_i + \delta RR_{i+1}).$$

Hence, considering decelerations larger than Δ_D, the averaging process of the PRSA method can be approximated as follows:

$$\begin{aligned} DC_{\mathbf{D}} &= \frac{1}{4}[\sum_{\Delta_I \geq \Delta_D} \sum_{\Delta_K} (\Delta_K + \Delta_I) A_{KI} \\ &+ \sum_{\Delta_I \geq \Delta_D} \sum_{\Delta_J} (\Delta_I + \Delta_J) A_{IJ}]. \end{aligned} \quad (2)$$

In particular, we assume $\Delta_D = 40$ ms, as this RR-increment corresponds to 5% of the average RR-interval.

For each adjacency matrix $\mathbf{A}$, a transition matrix $\mathbf{T}$ can be introduced which describes the conditional probability of observing Δ_J if an increment Δ_I has taken place:

$$T_{IJ} = \frac{A_{IJ}}{\sum_J A_{IJ}} = P(\Delta_J | \Delta_I). \quad (3)$$

Matrix $\mathbf{T}$ can also be interpreted as a directed and weighted network with the same vertices as in the matrix $\mathbf{A}$, but now the edges reflect probabilities of transitions from a given vertex.

Transition matrix $\mathbf{T}$ models a Markov process which underlies changes in the system studied. Matrix $\mathbf{T}$ is right stochastic, and consequently its stationary state can be inferred. This stationary state μ is the eigenvector of $\mathbf{T}$, corresponding to eigenvalue 1. Consequently, we can calculate the so-called entropy rate as follows:

$$S_{\mathbf{T}} = -\sum_{I=-K}^{K} \mu_I \sum_{J=-K}^{K} T_{IJ} \ln T_{IJ}. \quad (4)$$

2.4. Numeric and statistics methods

The estimates of $\mathbf{A}$ and $\mathbf{T}$ were obtained directly, by our own programmes. The statistical tests were performed using SigmaPlot 13.0 (Systat Software Inc.).

3. Results

The resulting graphs of networks are very large — sparse at the boundary states of equation (1) and approaching completeness around the vertex 0, namely for $|\Delta_J| < 100$ ms. This structure makes the presentation of the whole network difficult. Therefore, the networks are shown as contour plots of matrices limited to the transitions between RR-increments for $|\Delta_J| < 100$ ms.

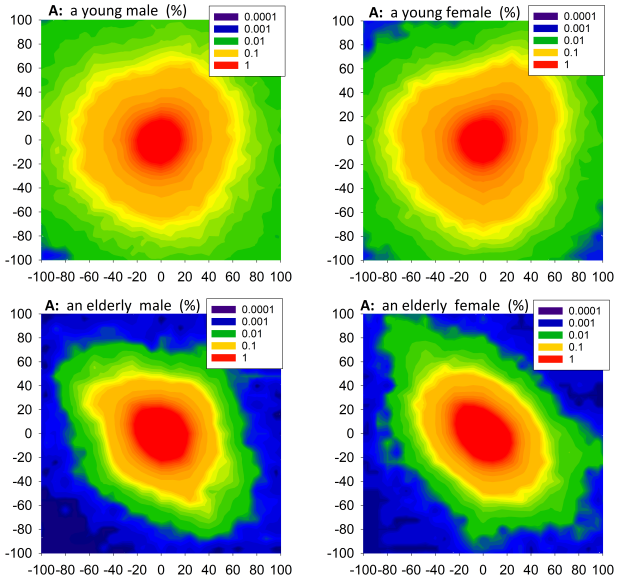

Figure 1. Adjacency matrices for diurnal activity: young (top) versus elderly (bottom), and males (left) versus females (right). The horizontal axes enumerate Δ_I; the vertical axes enumerate Δ_J of $A_{IJ} = P(\Delta_I, \Delta_J)$.

In the series of Figures 1, 2, 4 and 5, we show the mean adjacency matrices $\mathbf{A}$ and the mean transition matrices $\mathbf{T}$, estimated by pooling the matrices obtained from individual signals into the respective age-gender groups.

The diurnal events are well represented by $|\Delta_J| < 100$ intervals. The plots describe more than 91.4% of events for young males in a day, and up to 99.6% of events for elderly males in a day. But in the case of the nocturnal signal for the groups of young subjects, these parts of networks correspond to only 77.3% of transitions for males, and 85.2% of transitions for females. Therefore, the nocturnal networks for the groups of young subjects are presented in a different scale.

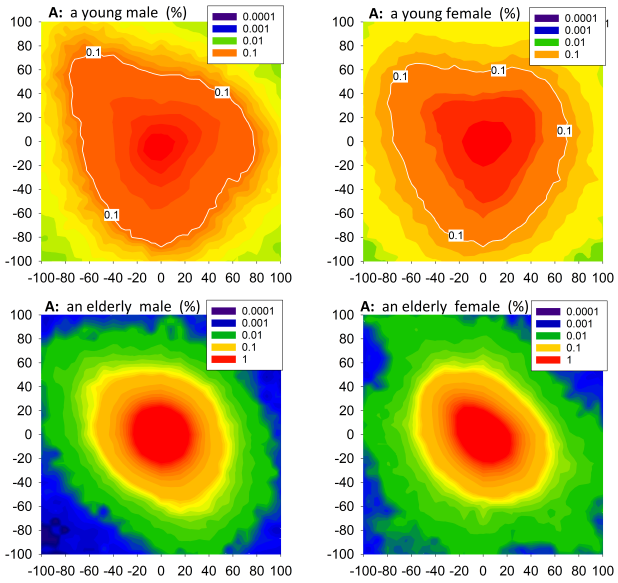

Figure 2. Adjacency matrices for nocturnal activity: young (top) versus elderly (bottom), and males (left) versus females (right). The horizontal axes enumerate Δ_I; the vertical axes enumerate Δ_J of $A_{IJ} = P(\Delta_I, \Delta_J)$.

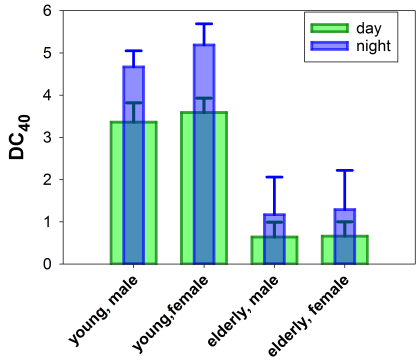

Figure 3. Mean deceleration capacity and its standard error obtained from matrices $\mathbf{A}$, pooled into the groups considered.

From Figures 1 and 2, we see that all probability distributions sharply peak around the most probable transition $(0,0)$. The $(0,0)$ transition represents the three identical RR-intervals occurring consecutively. However the probability of the $(0,0)$ transition is significantly different in age and circadian groups. It appears that:
$P^{day}_{young,m}(0,0)$=2.8 $\pm$0.6%, $P^{day}_{young,f}(0,0)$=3.2$\pm$0.7%, $P^{night}_{young,m}(0,0)$=0.7$\pm$0.1%, $P^{night}_{young,f}(0,0)$=1.00$\pm$0.3%, $P^{day}_{elderly,m}(0,0)$=7.8$\pm$1.3%, $P^{day}_{elderly,f}(0,0)$=7.0$\pm$1.1%, $P^{night}_{elderly,m}(0,0)$=4.1$\pm$ 0.6%, $P^{night}_{elderly,f}(0,0)$=4.3$\pm$0.9%. Furtermore, the way in which the distributions decay while

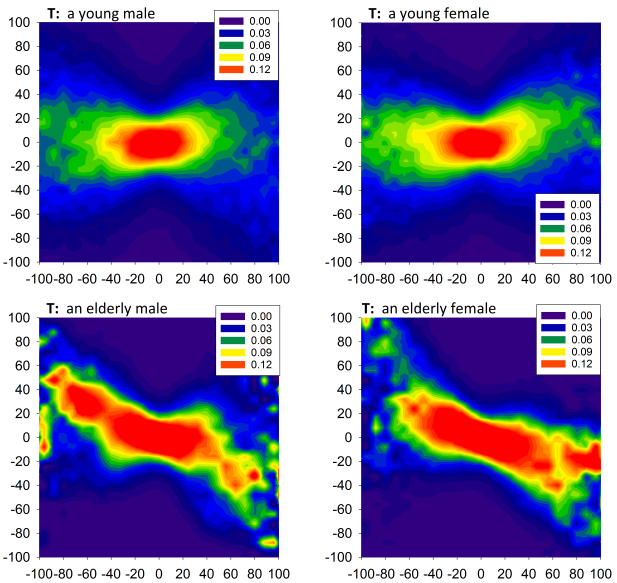

Figure 4. Transition matrices for diurnal activity: young (top) versus elderly (bottom), and males (left) versus females (right). The horizontal axes enumerate Δ_I; the vertical axes enumerate Δ_J of $T_{IJ} = P(\Delta_J|\Delta_I)$.

departing from the $(0,0)$ point strongly depends on the age and circadian rhythm. The influence of the gender is less evident.

The deceleration capacity $\mathbf{DC_{40}}$, shown in Figure 3, represents group properties related to large decelerations. We see systematic differences in the values of $\mathbf{DC_{40}}$ between nocturnal and diurnal rhythms. In the case of signals from the group of young subjects, this difference is statistically significant (t-test, male: P=0.035; female: P= 0.013). The gender differences are not significant.

From the transition matrices, plotted in Figures 4 and 5, in the case of diurnal dynamics in young subjects, we see that transition probabilities are only slightly dependent on the preceding event. However, in the case of the signals from elderly subjects, these transitions show antipersitency: after a deceleration, an acceleration is more probable, and vice verse.

Moreover, the nocturnal matrices are similar to the diurnal ones for the elderly, which might suggest that the sleep stages have less effect on their heart rhythm than in the young group. This may be related to the different sleep structure in the elderly — more light sleep and a relative decrease in or absence of deep sleep [6].

In the case of the elderly, the transition matrix shows a considerably more complex structure than for the young. In particular for the diurnal records, we can identify multiple 'islands' of transitions. In some cases these 'islands' are disjointed from the central core 'island' centred at (0,0). We hypothesize that these structures represent

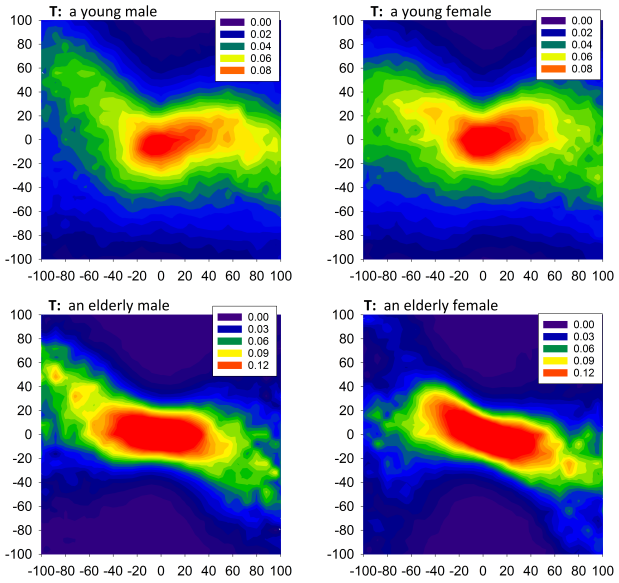

Figure 5. Transition matrices for nocturnal activity: young (top) versus elderly (bottom), and males (left) versus females (right). The horizontal axes enumerate Δ_I; the vertical axes enumerate Δ_J of $T_{IJ} = P(\Delta_J|\Delta_I)$.

pathological variability and are caused by possible occurrences of arrhythmias of various origins. The precise nature of this phenomenon requires further investigation.

The mean transition entropy resulting from the transition matrices presented in Figure 6 shows a systematic decrease. Moreover, for all groups the nocturnal transition entropy is higher than the diurnal in a one-sided t-test: P^{male}_{young} =0.001, $P^{female}_{elderly}$ =0.007, $P^{male}_{elderly}$ =0.026, $P^{female}_{elderly}$ =0.032. Gender differences are not significant.

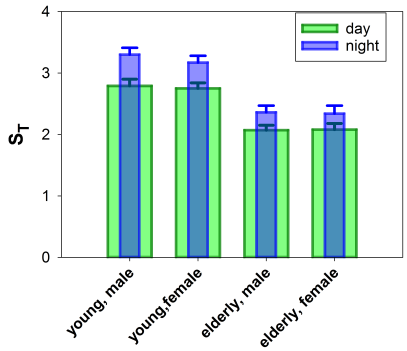

Figure 6. Mean transition entropy and its standard error obtained from matrices $\mathbf{T}$, pooled into the groups considered.

4. Conclusions

Large decelerations are considered to reflect the influence of high activity of the parasympathetic nervous system [2]. Therefore, we may see our results as showing that aging strongly diminishes vagal influence. Nevertheless, the higher vagal activity is related to the sleep time.

The methodological approach presented is capable of detailed characterization of the transition probability structure, as we demonstrate in an age and gender specific manner. In particular, we propose using our geometrically oriented approach for distinguishing between healthy and pathological variability. This may potentially aid the identification of arrhythmias of various origins, in addition to detailed characterization of the intrinsic complexity of heart rate.

Acknowledgements

The authors DM and ZRS acknowledge the financial support of the National Science Centre, Poland, UMO: 2012/06/M/ST2/00480.

The authors thank Dr Marta Zarczynska-Buchowiecka and Dr Joanna Wdowczyk of the Medical University of Gdansk for sharing the signals.

References

[1] Klabunde RE. Cardiovascular Physiology Concepts. Lippincott Williams & Wilkins, Wolters Kluwer, 2012.

[2] Poirier P. Exercise, heart rate variability, and longevity: the cocoon mystery? Circulation 2014;129(21):2085–2087.

[3] Campanharo ASLO, Sirer MI, Malmgren RD, Ramos FM, Amaral LAN. Duality between time series and networks. PLoS ONE 2011;6(8):e23378.

[4] Makowiec D, Kaczkowska A, Wejer D, Żarczyńska-Buchowiecka M, Struzik ZR. Entropic measures of complexity of short-term dynamics of nocturnal heartbeats in an aging population. Entropy 2015;17:1253–1272.

[5] Schumann AY, Bartsch RP, Penzel T, Ivanov PC, Kantelhardt JW. Aging effects on cardiac and respiratory dynamics in healthy subjects across sleep stages. Sleep 2010;33(07):943–955.

[6] Ohayon MM, Carskadon MA, Guilleminault C, Vitiello MV. Meta-analysis of quantitative sleep parameters from childhood to old age in healthy individuals: developing normative sleep values across the human lifespan. SLEEP 2004; 27(7):1255–73.

Address for correspondence:

Danuta Makowiec
Institute of Theoretical Physics and Astrophysics
University of Gdansk
ul Wita Stwosza 57, 80-952 Gdansk, Poland
fizdm@ug.edu.pl